Lithographic positioning of fluorescent molecules on high-*Q* photonic crystal cavities

Kelley Rivoire,[1,a] Anika Kinkhabwala,[2] Fariba Hatami,[3] W. Ted Masselink,[3] Yuri Avlasevich,[4] Klaus Müllen,[4] W. E. Moerner,[2] and Jelena Vučković[1]
[1]*Department of Electrical Engineering, Stanford University, Stanford, California 94305-4085, USA*
[2]*Department of Chemistry, Stanford University, Stanford, California 94305-4085, USA*
[3]*Department of Physics, Humboldt University, D-10115 Berlin, Germany*
[4]*Max-Planck Institute for Polymer Research, D-55124 Mainz, Germany*

(Received 5 July 2009; accepted 31 August 2009; published online 23 September 2009)

Photoluminescent molecules are coupled to high quality photonic crystal nanocavities. The cavities are fabricated in a gallium phosphide membrane and show resonances from 735 to 860 nm with quality factors up to 12 000. The molecules, which are dispersed in a thin polymer film deposited on top of the cavities, can be selectively positioned onto the location of the cavity by using a lithographic technique, which is easily scalable to arrays of cavities. © *2009 American Institute of Physics*. [doi:10.1063/1.3232233]

Photonic crystal nanocavities can confine light into volumes smaller than a cubic optical wavelength with extremely high quality factor, producing a strong interaction between light and emitters located in or near the cavity. These cavities have been used to demonstrate nanoscale on-chip devices and to probe fundamental quantum interactions between light and matter.[1–4] Experiments in this regime, however, are limited by the precision with which cavity and emitters can be spatially aligned and by the spectral range of emitters that can be coupled to cavity. Emitters are most often distributed randomly in the photonic crystal slab, and spatial alignment to the photonic crystal cavity occurs by chance. Recently, several techniques have been developed to position emitters with respect to cavities. These techniques rely primarily on either a mechanical transfer process to bring an emitter to the surface of the cavity[5,6] or the fabrication of a cavity at the location of a previously detected emitter.[7,8] Neither method is easily scalable to arrays of cavities and emitters, nor achievable with conventional semiconductor fabrication processes.

Coupled photonic crystal cavity-emitter systems studied so far are primarily based on gallium arsenide and silicon materials, which absorb strongly at wavelengths shorter than the electronic band gap of the material. This precludes the use of emitters such as organic molecules, which typically have resonances at visible wavelengths. Research in photonic crystals operating at these shorter wavelengths has used materials such as GaN (Ref. 9) and Si_3N_4.[10,11] These materials have a lower refractive index than GaAs or Si ($n \approx 2.4$ for GaN and $n \approx 2.0$ for Si_3N_4 compared to $n \approx 3.5$ for GaAs and Si), which limits the size of photonic band gap and has generally led to low experimental quality factors of up to a few thousand, although designs with higher quality factors (Q) (up to 1×10^6) have been proposed.[12] Previously, we demonstrated[13] that photonic crystal cavities with quality factors up to 1700, limited by fabrication inaccuracy, could be fabricated in gallium phosphide (GaP), a high-index III-V semiconductor with indirect band gap at 550 nm. The high index of the material enables a large photonic band gap and cavities with high quality factor, while the large electronic band gap prevents absorption in the near-IR and part of the visible. Here, we demonstrate cavities with quality factors above 10 000 at wavelengths compatible with near-IR fluorophores and show that we can selectively position these molecules on top of a nanocavity using conventional lithography techniques.

Our cavity is a linear three-hole defect (L3) (Ref. 14) fabricated in a 125 nm GaP membrane grown by gas-source molecular beam epitaxy. A scanning electron microscope (SEM) image of a fabricated cavity and the simulated electric field intensity of the fundamental high-Q cavity mode are shown in Figs. 1(a) and 1(b). Cavities are fabricated as described in a previous work.[13] The molecule we use is dinaphthoquaterrylene diimide (DNQDI),[15] which was chosen for its broadband emission over the desired wavelength range

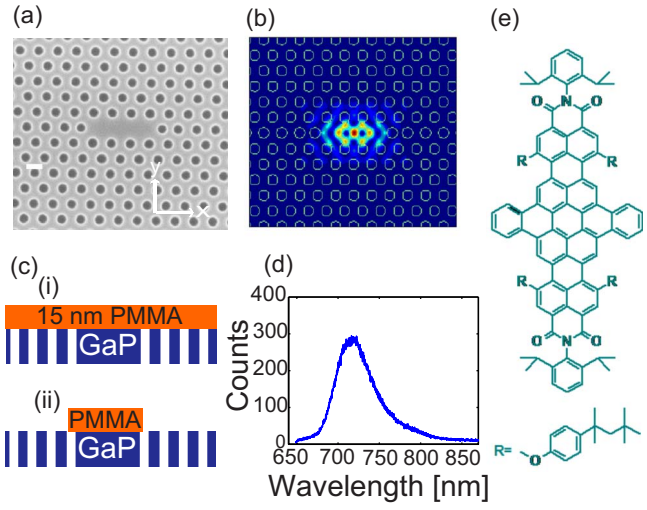

FIG. 1. (Color online) (a) SEM image of a fabricated photonic crystal cavity in GaP. Scale bar indicates 200 nm. (b) FDTD simulation of electric field intensity of the fundamental cavity mode. The mode is primarily $\hat{y}$-polarized (c) Schematic illustrating coupling of molecule to cavity. (i) DNQDI/PMMA is deposited over the entire structure. (ii) DNQDI/PMMA is lithographically defined on cavity region. (d) Bulk PL spectrum of DNQDI when excited with a 633 nm HeNe laser. The molecule has a peak in its absorption at this excitation wavelength. (e) Chemical structure of DNQDI molecule.

[a]Electronic mail: krivoire@stanford.edu.

(700–850 nm), good photostability, and high photoluminescence (PL) quantum yield (40%). The structure of the molecule and its emission spectrum are shown in Fig. 1. To couple DNQDI to photonic crystal cavities [Fig. 1(c)], the molecule was dissolved into a solution of 1% poly(methyl methacrylate) (PMMA) in distilled toluene. In standard lithographic processing, this solution is then spun onto a surface, leaving behind a smooth, thin film of dye-doped resist. However, spinning onto an uneven surface, such as a photonic crystal membrane, causes unwanted aggregation of the dye-doped PMMA. Instead, the solution was float-coated,[16] whereby the photonic crystal sample is submerged into a water bath and a single drop of the dye-doped PMMA in toluene solution is dropped onto the surface of the water bath. The drop quickly disperses across the surface leaving a locally uniform layer of hydrophobic dye-doped resist floating on top of the water bath. The water is then pipetted away, allowing the PMMA layer to fall on top of the photonic crystal sample. The sample is baked at 90 °C for 30 min to ensure that all the water is fully evaporated. The concentration of DNQDI in the PMMA layer is approximately 5 molecules/100 nm^2.

We first characterize cavities passively prior to depositing molecules. We probe cavity resonances using cross-polarized normal-incidence reflectivity with a tungsten halogen white light source.[13] The cross-polarization configuration is used to obtain a sufficient signal-to-noise ratio to observe the cavity resonance above the reflected background uncoupled to the cavity. A typical reflectivity spectrum is shown in Fig. 2(a), showing the multiple resonances of the L3 cavity; the fundamental mode is denoted with a black box. The spectrum of the fundamental mode [Fig. 2(b)] is fit to a Lorentzian, giving a quality factor of 10 000. (The improvement in quality factor from Ref. 13 is due to better fabrication.) After depositing the molecules over the entire structure, we measure PL of the molecule [Fig. 2(c)] using a 633 nm helium-neon excitation laser in a confocal microscope setup. Above the broad emission from molecules not coupled to the cavity, we observe sharp polarized resonances identical to those in our reflectivity measurements, demonstrating the molecules are coupled to the cavity modes. The quality factor of the fundamental mode is measured to be 10 000, indicating that deposition of molecules onto the membrane does not degrade the properties of the cavity, in agreement with finite difference time domain simulations for a thin (<40-nm-thick) layer of PMMA. After deposition of molecules, we observe a small (several nanometers) redshift in the cavity resonance, as expected from simulations. With no DNQDI/PMMA present, only background counts are detectable over the entire spectral range. We vary the spatial periodicity of the photonic crystal holes and hole radius to tune the fundamental cavity resonance through the PL spectrum of the molecule. We measure high cavity quality factors up to 12 000 via PL [Fig. 2(d)] across a range of more than 100 nm, from 735 to 860 nm. The cavity Q is higher at longer wavelengths, where we fabricate most of our cavities, as fabrication imperfections are reduced because the feature size is larger. Small differences in cavity Q between reflectivity and PL measurements [Fig. 2(d))] are primarily due to fit error. Since the molecules are doped into PMMA, an electron-beam lithography resist, it is straightforward to selectivity expose and develop the resist using e-beam lithography[17] so molecules and PMMA remain only at the location of the photonic crystal cavity [Fig. 1(c)]. The size of the unexposed region at the center of the photonic crystal cavity is approximately 700×400 nm^2. While float-coating deposits resist uniformly over a small region, PMMA thickness variations were observed from one coating to the next, so electron-beam doses were varied for different cavities on one sample. Figure 3(a) shows a scanning confocal image of PL from a photonic crystal cavity coated with DNQDI-doped PMMA. The PL is flat to within 3.5%, with slightly more emission from the cavity region, likely a result of enhanced outcoupling from molecules coupled to the cavity mode. Figure 3(b) shows PL from the same cavity, measured with the same excitation power, after electron-beam exposure and removal of the resist surrounding the cavity. There is still strong emission, though diminished by the e-beam process, from the cavity region, but there is no emission from the nearby areas, so the contrast is much larger. Figure 3(c) shows a PL spectrum (Q=4500) measured on the same cavity after localization of the resist to the cavity, demonstrating that molecules are spectrally coupled to photonic crystal cavity. An atomic force microscope image [Fig. 3(d)] confirms that DNQDI-doped PMMA is localized to the cavity and is 12 nm in height. The atomic force microscope image shows a misalignment of approximately 300 nm between the cavity region and the lithography defined DNQDI/PMMA region. With optimization of the overlay process, it should be possible to reduce this error to less than 50 nm.

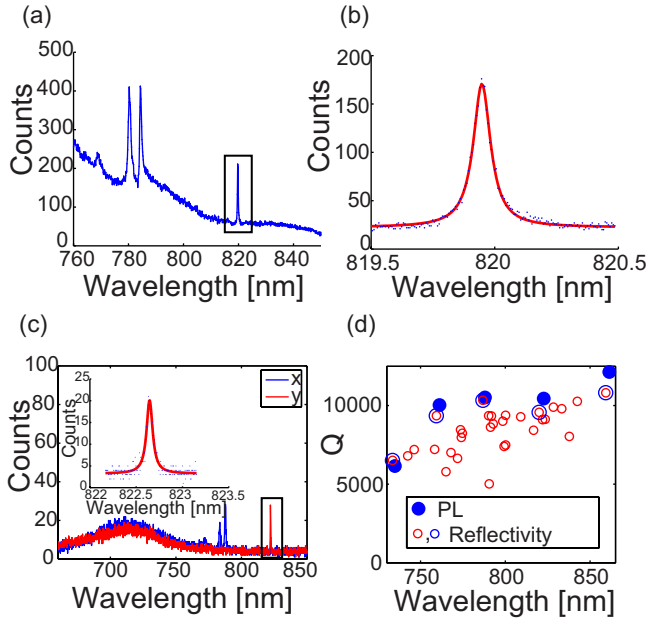

FIG. 2. (Color online) (a) Cross-polarized reflectivity measurement of a cavity. The box indicates fundamental cavity mode. (b) Reflectivity spectrum of high quality factor fundamental cavity mode [box in (a)] Spectrum shows additional peaks at shorter wavelengths from higher order cavity modes. Solid line shows Lorentzian fit with quality factor 10 000. (c) PL collected from the same photonic crystal cavity in (a) and (b) after molecules are deposited on cavity. x-polarized emission is shown in blue; y-polarized emission is shown in red. Inset: PL measurement of fundamental cavity mode (black box). Line indicates Lorentzian fit with Q=10 000. (d) Quality factors measured from reflectivity before molecule deposition and PL after molecule deposition from the high-Q cavity mode for structures with lattice constant a and hole radius r/a tuned so that the fundamental cavity resonance shifts across the PL spectrum of the molecule. Blue open circles indicate reflectivity measurements for the cavities that were also measured in PL (blue closed circles).

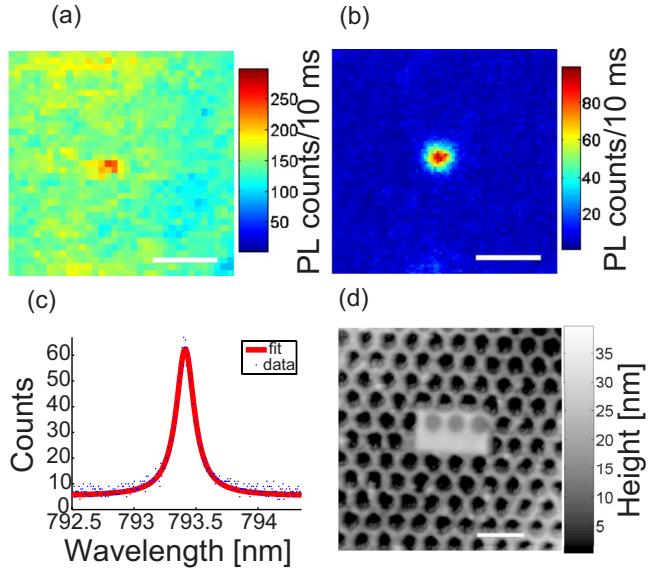

FIG. 3. (Color online) (a) Scanning confocal image of PL from DNQDI doped PMMA float-coated onto a photonic crystal membrane. Pixel size is 200 nm and scale bar indicates 2 μm. (b) Scanning confocal image of DNQDI PL after electron-beam lithography is used to remove all molecules, except for the ones coating the cavity region at the center. The same imaging laser power as in (a) was used. Pixel size is 80 nm and scale bar indicates 2 μm. (c) PL spectrum from the fundamental mode of photonic crystal cavity after selective removal of molecules by e-beam lithography. (d) Atomic force microscopy image showing localization of DNQDI-doped PMMA to the cavity region. PMMA thickness is 12 nm. Scale bar indicates 500 nm.

In conclusion, we have demonstrated the coupling of fluorescent molecules and photonic crystal cavities with resonances in the far-red and near-infrared wavelengths and quality factors up to 12 000. By exposing and developing the molecule's polymer host using electron-beam lithography, we localize the molecule to the cavity region. Our results show that molecules can be coupled to high quality factor photonic crystal cavities and easily localized to the spatial location of the nanoscale cavity using standard lithographic techniques.

Financial support was provided by the National Science Foundation (NSF Grant Nos. DMR-0507296 and DMR-0757112) and the Stanford Center for Probing the Nanoscale (through NSF Grant No. PHY-0425897). K.R. is supported by the National Science Foundation Graduate Research Fellowship and a Stanford Graduate Fellowship. The work was performed in part at the Stanford Nanofabrication Facility of NNIN. K. Rivoire and A. Kinkhabwala are equal contributors to this work.

[1] S. Noda, M. Fujita, and T. Asano, Nat. Photonics **1**, 449 (2007).
[2] D. Englund, A. Faraon, I. Fushman, N. Stoltz, P. Petroff, and J. Vučković, Nature (London) **450**, 857 (2007).
[3] T. Yoshie, A. Scherer, J. Hendrickson, K. Khitrova, H. Gibbs, G. Rupper, C. Ell, O. Shchekin, and D. Deppe, Nature (London) **432**, 200 (2004).
[4] H. Altug, D. Englund, and J. Vučković, Nat. Phys. **2**, 484 (2006).
[5] M. Barth, N. Nusse, B. Lochel, and O. Benson, Opt. Lett. **34**, 1108 (2009).
[6] P. Barclay, C. Santori, K.-M. Fu, R. Beausoleil, and O. Painter, Opt. Express **17**, 8081 (2009).
[7] K. Hennessy, A. Badolato, M. Winger, D. Gerace, M. Atature, S. Gulde, S. Falt, E. Hu, and A. Imamoglu, Nature (London) **445**, 896 (2007).
[8] S. Thon, M. Rakher, H. Kim, J. Gudat, W. Irvine, P. Petroff, and D. Bouwmeester, Appl. Phys. Lett. **94**, 111115 (2009).
[9] Y.-S. Choi, K. Hennessy, R. Sharma, E. Haberer, Y. Gao, S. DenBaars, S. Nakamura, and E. Hu, Appl. Phys. Lett. **87**, 243101 (2005).
[10] M. Barth, J. Kouba, J. Stingl, B. Lochel, and O. Benson, Opt. Express **15**, 17231 (2007).
[11] M. Makarova, J. Vučković, H. Sanda, and Y. Nishi, Appl. Phys. Lett. **89**, 221101 (2006).
[12] M. McCutcheon and M. Lončar, Opt. Express **16**, 19136 (2008).
[13] K. Rivoire, A. Faraon, and J. Vučković, Appl. Phys. Lett. **93**, 063103 (2008).
[14] Y. Akahane, T. Asano, B. Song, and S. Noda, Nature (London) **425**, 944 (2003).
[15] Y. Avlasevich, S. Muller, P. Erk, and K. Mullen, Chem.-Eur. J. **13**, 6555 (2007).
[16] H. Zhou, B. Chong, P. Stopford, G. Mills, A. Midha, L. Donaldson, and J. Weaver, J. Vac. Sci. Technol. B **18**, 3594 (2000).
[17] L. Martiradonna, T. Stomeo, M. D. Giorgi, R. Cingolani, and M. D. Vittorio, Microelectron. Eng. **83**, 1478 (2006).